Pergamon

PII: S1359-6454(96)00394-1

MODELING OF NON-UNIFORM SPATIAL ARRANGEMENT OF FIBERS IN A CERAMIC MATRIX COMPOSITE

S. YANG, ASIM TEWARI and ARUN M. GOKHALE

Department of Materials Science and Engineering, Georgia Institute of Technology, Atlanta, GA 30332-0245, U.S.A.

Abstract—In the unidirectional fiber reinforced composites, the spatial arrangement of fibers is often non-uniform. These non-uniformities are linked to the processing conditions, and they affect the properties of the composite. In this contribution, a recently developed digital image analysis technique is used to quantify the non-uniform spatial arrangement of Nicalon fibers in a ceramic matrix composite (CMC). These quantitative data are utilized to develop a six parameter computer simulated microstructure model that is statistically equivalent to the non-uniform microstructure of the CMC. The simulated microstructure can be utilized as a RVE for the micro-mechanical modeling studies. © 1997 Acta Metallurgica Inc.

INTRODUCTION

The properties and performance of unidirectional aligned fiber reinforced composites depend on the metric geometric attributes of the fibers such as volume fraction, number density, size distribution, etc., *and* spatial arrangement of fibers in the matrix. Usually, the spatial arrangement of fibers is not uniform. Figure 1 shows the microstructure of a ceramic matrix composite (CMC) containing uni-directional aligned SiC fibers (Nicalon) in a glass ceramic (MAS) matrix. The spatial distribution of fibers appears to be non-uniform, and there is a distribution of fiber sizes. The non-uniform nature of the spatial distribution of fibers is usually linked to the processing techniques used for making the composites.

Recently, Brockenbrough *et al.* [1] showed that, in the plastic regime, the transverse deformation of metal matrix composites is significantly affected by non-periodic spatial distribution of fibers. These authors concluded that the theories and models based on periodic spatial distribution of brittle fibers in a ductile matrix cannot correctly predict the transverse deformation behavior of the composites having non-uniform spatial distribution of fibers. Sorensen and Talreja [2] studied various non-uniformities of fiber distributions systematically and found that the local residual stresses due to cool-down during processing depend significantly on deviations from uniformity of spatial distributions of fibers. They also showed that in assessing the effects of coatings and interphases such non-uniformities must be taken into account [3]. Pyrz [4, 5] observed that in a polymer matrix composite, the transverse constitutive behav-ior and fracture path tortuosity are sensitive to the

spatial arrangement of fibers, which in turn depends on the material's processing parameters. Whited *et al.* [6] observed that micro-crack damage evolution during thermal cycling of MMC is quite sensitive to the inter-fiber distances.

The above discussion shows that: (1) the micro-structure of composites often consists of non-uniform spatial distributions of fibers; (2) the non-uniformities in the spatial arrangement of fibers are governed by the techniques and parameters used for material processing; and (3) plastic deformation, damage evolution and fracture of composites depend on the spatial distribution of fibers. Therefore, it is of interest to develop quantitative models for the microstructure of fiber composites that account for the non-uniform spatial distribution of fibers. An appropriate microstructural model can provide an important input for the virtual integrated prototyping of the composite manufacturing process. In this context, it is important to point out that the spatial distribution of fibers may vary from batch to batch, or from one plate to another plate of the same batch, and some times, from one region to another region in the same plate.

The current approaches to the micro-mechanical modeling of the behavior of composites do not consider the non-randomness and non-uniformity of the spatial distribution of fibers. Therefore, there is a need to develop a micro-mechanical modeling approach, where the representative volume element (RVE) represents the real composite microstructure. Such a modeled microstructural volume element should have the same volume fraction, number density and size distribution of fibers as in the real composite, *and* the spatial distribution of fibers should be *statistically* equivalent to that in the

microstructure of the composite. Therefore, the modeled microstructure can be used to generate the RVE for micro-mechanical modeling studies.

The modeled microstructure can provide a vital input for virtual integrated prototyping of the CMC manufacturing process. The parameters of the model can be changed to simulate statistically different microstructures arising from the same basic manufacturing process but under different process parameters. This should be particularly useful where the spatial distribution of the fibers varies from one batch to another. The effect on the mechanical behavior can
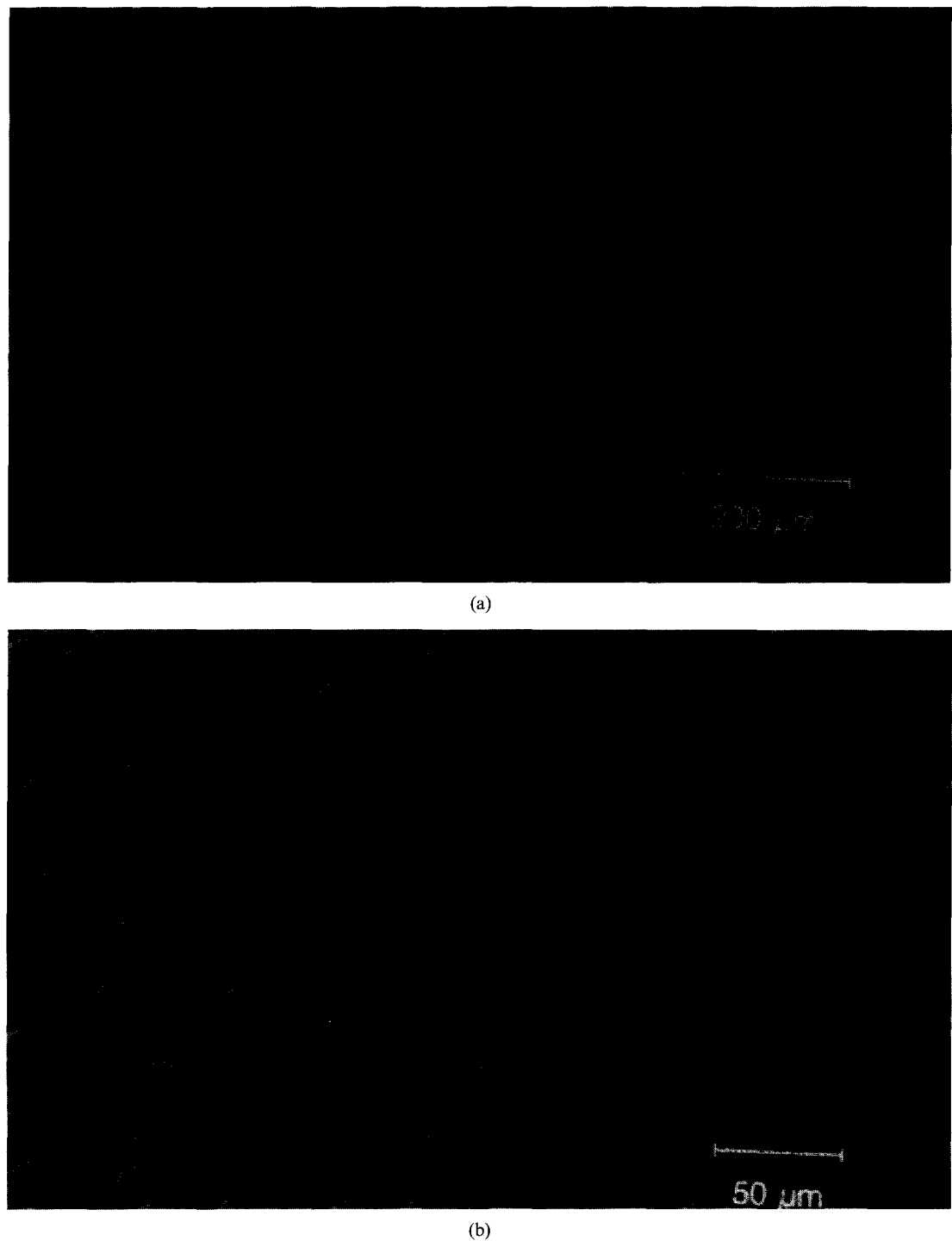

(a)

(b)

Fig. 1. Microstructure of a ceramic matrix composite having unidirectional aligned Nicalon fibers in a glass ceramic matrix. (a) Low magnification micrograph showing fiber-rich and fiber-poor regions. (b) High magnification micrograph illustrating size distribution and local spatial arrangement of fibers.

then be investigated through the micro-mechanical modeling approach.

It is the purpose of this contribution to present a methodology that enables the development of a quantitative microstructure model for unidirectional aligned fiber reinforced CMC, where the fibers are non-uniformly distributed. The next section gives a brief background to two important statistical distributions that quantify the spatial arrangement of fibers. The subsequent section describes the experimental technique for an *unbiased* estimation of these distribution functions, and that is followed by the interpretation of the measured spatial descriptors. Finally, a geometric model is developed for the non-uniform spatial arrangement of fibers observed in a CMC, and it is shown that the spatial arrangement of fibers in the modeled microstructure is statistically equivalent to that in the CMC.

BACKGROUND

The theoretical statistics literature contains a large number of contributions that deal with the statistics of spatial *point patterns* (not finite size particles or fibers), and the quantitative descriptors that reflect various attributes of these patterns [7, 8]. There are a large number of distance distribution functions that can be used to quantify different aspects of the spatial arrangement of fiber centers. In the present work, the nearest neighbor distribution function and radial distribution function are utilized to quantify the spatial arrangement of fiber centers.

The nearest neighbor distribution function provides quantitative information on the spatial arrangement of fiber centers in the immediate vicinity of a typical fiber [9-11]. The radial distribution function [7, 8, 12-14] reflects quantitative information concerning the long range, the intermediate range and the short range spatial arrangement as a function of distance from a typical fiber. These descriptors are useful to characterize overall spatial clustering, repulsion or randomness of the population of fibers.

The nearest neighbor distribution function [9-11] is given by the probability density function $\psi(r)$ such that $\psi(r)dr$ is equal to the probability that there is no fiber center in a circle of radius r around a typical fiber, and there is at least one fiber center in the circular shell of radii r and $(r + dr)$. The nearest neighbor distribution function can be experimentally measured by measuring the nearest neighbor distances of a large number of fibers sampled in an *unbiased* manner.

Let N be the number of fiber centers in the metallographic plane of area A. The *average* number of fiber centers per unit area N_A is equal to $[N/A]$. Draw a circular shell of radii r and $(r + dr)$ around the ith fiber whose centroid is at coordinates (X_i, Y_i), and count the number of fiber centers in this circular shell. Repeat the measurement by placing the circular shell around a large number of fibers (say, $i = 1$,

2,..., N). Calculate the average number of fiber centers in a circular shell of radii r and $(r + dr)$ around a typical fiber, and divide it by $[2\pi r N_A dr]$: the ratio is equal to the value of the radial distribution function at a distance of r. The radial distribution function at difference values of distances r can be estimated by repeating the measurements for the shell of various sizes. Formally, the radial distribution function, $G(r)$ is defined as follows [7, 8, 12-14]

$$G(r) = \frac{1}{2\pi r N_A} \cdot \frac{dK(r)}{dr}. \tag{1}$$

$dK(r)$ is the average number of fiber centers in a circular shell of radii r and $(r + dr)$ around a typical fiber. Note that for randomly distributed *points* (not fibers of finite size) having number density N_A, the average number of points in the circular shell around any point is equal to $[2\pi r N_A dr]$. Therefore, for a set of randomly distributed *points*, $G(r)$ is equal to 1. It is important to point out that for a population of finite size fibers, a value of $G(r)$ higher than 1 does not necessarily imply that the fibers are clustered. This is because, as demonstrated in a subsequent section, the radial distribution function of the finite size fibers depends on the spatial arrangement of the fiber centers, *and* the fiber volume fraction, average size, etc. It is also important to point out that the radial distribution function for any arbitrary spatial arrangement approaches 1, as $r \to \infty$. This is because at sufficiently large distances, the shell area $[2\pi r dr]$ becomes so large that it automatically averages over all possible variations, consequently, in equation (1), $dK(r) \to N_A[2\pi r dr]$, as $r \to \infty$, and therefore, $G(r) \to 1$, as $r \to \infty$.

EXPERIMENTAL MEASUREMENT OF SPATIAL DISTRIBUTIONS

The experimental measurement of nearest neighbor distribution function or radial distribution function involves measurements of distances between fiber centers in a metallographic plane perpendicular to the fibers. For this purpose, it is necessary to observe the microstructure at a reasonably high magnification, where the individual fibers can be clearly resolved, and the fiber sizes and the inter-fiber distances can be accurately measured. At such magnifications (typically from 100 × to 500 × depending on average fiber size) the microstructure is observed one field of view at a time; each field of view or microstructural frame represents a small area of the metallographic plane. Unfortunately, there are serious problems associated with reliable and unbiased estimation of the spatial distribution functions when the microstructure is observed field by field, i.e. one field at a time. Some difficulties are listed below.

(1) The nearest neighbor of a given fiber may *not* be in the same field of view [see Fig. 2(a)]. Therefore, measuring the nearest neighbor distances from individual microstructural fields
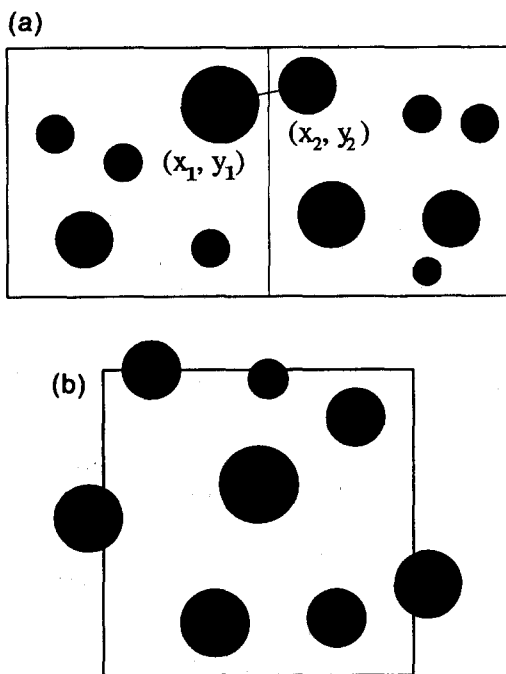
(a)

(b)

Fig. 2. (a) Example of a fiber that has a nearest neighbor in the adjoining field. (b) Due to the presence of edges, the fibers on the frame boundaries are partly-in–partly-out; their centers may be in the adjoining field.

or micrographs *cannot* provide the data for reliable and unbiased estimation of the nearest neighbor distribution function. The error and bias are even larger for the higher order neighbors.

(2) Some fibers are always present on the "edges" of the microstructural field or micrograph. Such fibers are "partly in and partly out", and their centroids may not be in the field of view under observation [see Fig. 2(b)]. Ignoring such fibers can create a serious systematic error (*bias*), in both the radial distribution and nearest distribution function, because larger fibers are more likely to intersect the frame boundaries.

(3) Measurement on individual fields restricts the estimation of radial distribution function to the distances typically less than one fourth of the size of the microstructural frame. Therefore, reliable information about intermediate and long range spatial patterns cannot be obtained from such data.

The above difficulties are due to the "edge effect", which can be eliminated by eliminating the edges! Digital image analysis offers a practical solution to this problem. It is possible to create a "montage" of

†The process is equivalent to (but a lot more efficient and accurate than) taking (say) 25–50 micrographs of contiguous microstructural frames, matching the borders, and pasting them together on a large board.

perfectly matching (within one pixel) large number of adjoining contiguous microstructural fields (say, 100 or more microstructural frames) in the memory of the digital image analyzer†. The software based procedure for creating such an image montage is described in detail in another contribution [12]. Once such a montage is created, the "edges" are eliminated for all practical purposes, and it is possible to obtain the (X, Y) centroid coordinates [referred to the same $(0, 0)$ origin] and size of the fibers in the montage, through digital image analysis procedures. The image segmentation procedure to separate the touching fibers and to correctly identify each individual fiber is described elsewhere [15]. From the data on (X, Y) centroid coordinates of the fibers in the montage referred to the same $(0, 0)$ origin, one can then calculate the distance between any two fibers in the montage, that may or may not be in the same microstructural field (see Fig. 3).

Calculation of spatial distribution functions from image analysis data

The raw data from image analysis consist of a string of numbers for each fiber representing (X, Y) centroid coordinates, size, shape, perimeter, etc. Typically, each set will consist of these data on about 500–1000 fibers. The radial distribution function and nearest neighbor distribution function can be calculated from such a data set through appropriate computer codes. These calculations involve operations on reasonably large data sets, and require extensive number crunching. For example, to calculate the radial distribution function, a circular shell of radii r and $(r + \Delta r)$ is placed at the center of the ith fiber and the number of other fiber centroids inside this shell are counted. This essentially amounts to identifying all the fiber centers that are in the distance range r to $(r + \Delta r)$ from the given fiber located at (X_i, Y_i). The test shell is then placed at the center of the next fiber and the count is repeated. The procedure is then continued for all the fibers (say, $i = 1$–1000); the average value of this quantity yields the radial distribution function for that value of r. The procedure is then repeated for different r values to generate the complete radial distribution function.
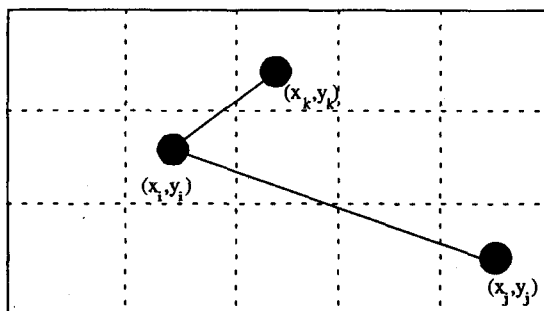

Fig. 3. Creation of montage eliminates edge effects for all practical purposes, and distances between fibers that may be in different microstructural fields can be measured.
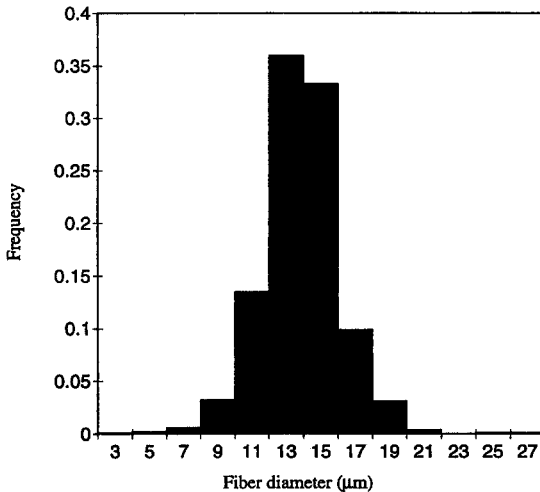
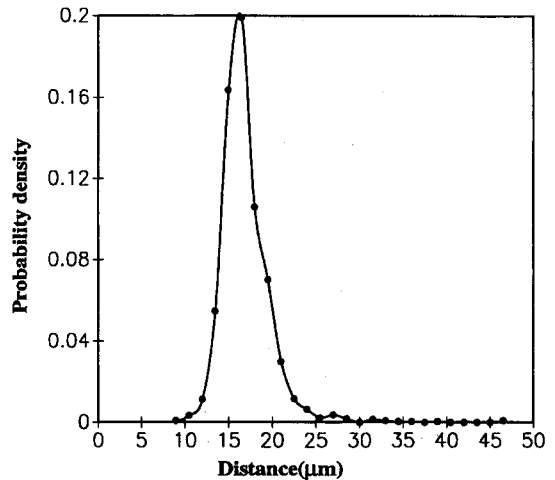Fig. 4. Size distribution of SiC fibers (Nicalon) in a histogram form.

Fig. 5. Experimentally measured nearest neighbor distribution function of the SiC fiber centers in the CMC.

Spatial distribution functions of SiC fibers in a ceramic matrix composite

The above experimental procedure was applied to estimate the radial distribution function and the nearest neighbor distribution function of unidirectional aligned SiC fibers in a CMC, whose microstructure is shown in Fig. 1. Figure 4 shows the size distribution of the fibers. The volume fraction of the fibers is 0.35, the average fiber diameter is 14 μm, and the size distribution can be represented by a normal distribution. The spatial distributions were estimated from the "montage" of 60 fields of view observed at 500 × . The "montage" covered an area of 1.25 mm^2 on the metallographic specimen in the form of a strip. The montage contained about 2500 fibers. Each data point on the radial distribution is an average obtained by placing the circular shell around at least 1000 fibers. It is important to emphasize that extensive sampling is necessary to obtain a statistically representative and reliable radial distribution function. Figure 5 shows the nearest neighbor distribution function of the SiC fibers, and Fig. 6 presents the radial distribution function of the SiC fibers. Note that the first peak of the radial distribution function is quite high, and there is a small but consistent dip below 1 at large distances. It will be shown in the next section that these observations imply short range clustering and long range scarcity of fibers.

COMPUTER SIMULATION OF HARD-CORE RANDOM FIBER ARRANGEMENTS AND INTERPRETATION OF SPATIAL DISTRIBUTIONS

To quantify the deviations of spatial arrangement of fiber centers from uniformity and randomness, it is necessary to compare the experimental spatial arrangement with that for a "uniform" distribution of fibers. Strictly speaking, the spatial distribution of

fiber centers *cannot* be random (i.e. Poisson) if the fibers are of non-zero (finite) size. This is because, for a completely random spatial distribution, the probability of finding a fiber center should be exactly the same in any infinitesimal region of the microstructure. This condition cannot be satisfied in a real microstructure having fibers of non-zero size, because the probability of finding a fiber center inside another fiber is obviously zero, and it is not zero outside the fiber. Therefore, there can be a random distribution of zero dimensional points only. For a random distribution of points in a plane, the radial distribution function is equal to one, and the nearest neighbor distribution can be calculated analytically [11]. For the fibers of finite size, the "base line" or most uniform spatial distribution is what is called the "hard-core random" distribution, which can be computer simulated, but there are no analytical
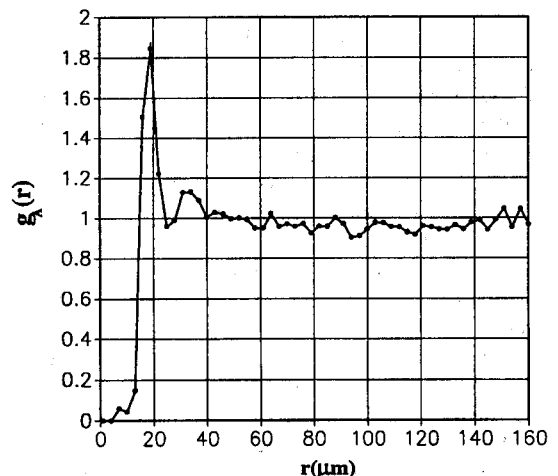

Fig. 6. Experimentally measured radial distribution function of SiC fiber centers in the CMC.

equations for the radial distribution function or the nearest neighbor distribution function for such a spatial arrangement.

The hard-core random distribution of finite size unidirectional aligned fibers can be simulated in a straight-forward manner. A random number generator is used to select a random point in a plane perpendicular to fibers, and a fiber of given size is "placed" at that location. Another random point is selected, if this point does not lie inside the first fiber, then a second fiber is placed at this location. If the second random point lies inside the first fiber then it is discarded, and another random point is generated. The process is repeated until the required number density, volume fraction and size distribution of fibers are generated. The nearest neighbor distribution and radial distribution functions of such simulated hard-core random microstructures can be calculated by averaging over a *large* number of realizations.

The spatial distribution functions of the simulated hard-core random population of fibers depend significantly on the fiber volume fraction, number density, average size and standard deviation of the size distribution of fibers. Figure 7(a) shows the calculated radial distribution of a computer simulated hard-core random structure for different fiber volume fractions. For this simulation, all the fibers are of 14 μm diameter (which is the average size of SiC fibers in the CMC). Note that the radial distribution function varies significantly with the fiber volume fraction. The height of the first peak increases with the increase in the fiber volume fraction. Figure 7(b) depicts the nearest neighbor distribution function for the same hard-core random simulations. Note that the nearest neighbor distribution depends significantly on the fiber volume fraction. Figure 8(a) illustrates the effect of the spread in the fiber sizes (standard deviation σ) on the radial distribution function for hard-core random arrangement of fibers of normal size distribution, same volume fraction (0.35) and the same average size (14 μm). The height of the first peak and the width are particularly sensitive to the standard deviation (σ) of the normal fiber size distribution. The nearest neighbor distribution of fibers [Fig. 8(b)] is also sensitive to the standard deviation of the fiber size distribution. Figure 9 shows three distinctly different fiber size distributions that have the same average fiber size and standard deviation: these size distributions have different skewness. Figure 10 shows the spatial distributions of the simulated hard-core random arrangements corresponding to the size distributions in Fig. 9. The radial distribution and the nearest neighbor distribution do *not* vary with the skewness of the fiber size distribution!

The simulation studies clearly demonstrate that to quantify and interpret the deviations from uniformity, it is imperative that the experimental spatial distributions be compared with the simulated
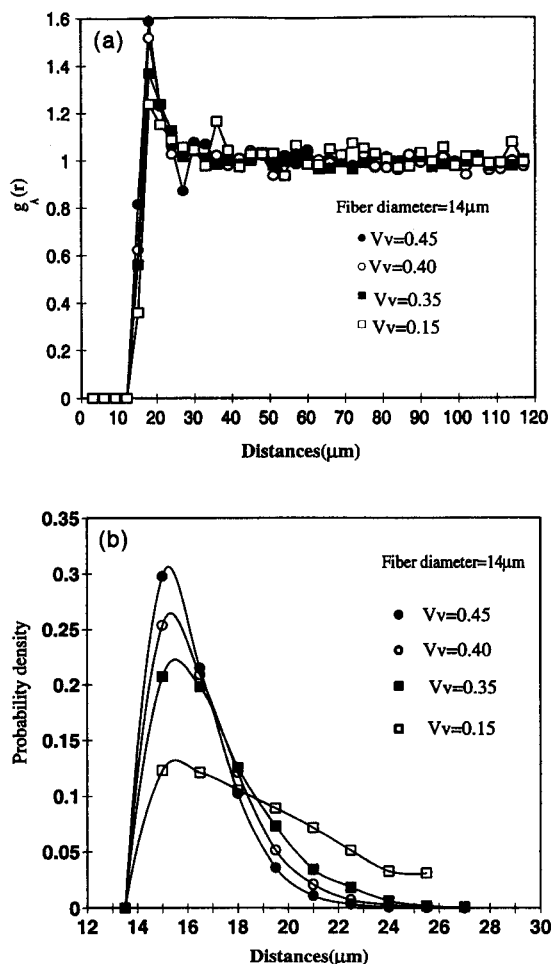

Fig. 7. Spatial distribution functions of randomly distributed monosize fibers in simulated microstructure with hard-core model. (a) Radial distribution functions of randomly distributed monosize fibers at different fiber volume fractions. (b) Nearest neighbor distribution functions of randomly distributed monosize fiber at different volume fractions.

hard-core random spatial distributions that have the same volume fraction, average fiber size and standard deviation of the fiber size distribution. Any conclusions regarding the deviations from randomness that are not based on such a comparison need to be re-examined. Figure 11(a) compares the experimentally radial distribution function of the SiC fibers in the CMC with the corresponding radial distribution function for simulated hard-core random fiber population having the same volume fraction and size distribution of fibers. Note that the first peak in the experimentally measured distribution is significantly higher than that in the hard-core random structure, although the peak positions are approximately the same. Let P_e be the height of the first peak of the experimentally measured radial distribution function of the SiC fibers, and let P_r be the height of the first peak for the corresponding simulated hard-core random distribution. To quantify the extent of

short-range clustering, a clustering parameter C_s can be defined as follows.

$$C_s = P_e/P_r. \tag{2}$$

For the present composite, C_s is equal to 1.33. Therefore, in the CMC, at short distances, there are about 33% more fiber centers in a given area around a typical fiber, as compared to that in the hard-core random structure.

For hard-core random structure, the radial distribution is equal to 1.0, soon after the first peak, irrespective of the fiber volume fraction or size distribution of fibers [see Figs 7(a), 8(a) and 10(a)]. The experimentally measured distribution is consistently below 1.0 for distances ranging from 50 to 140 μm, and then it increases and settles at 1.0 at very large distances. The long distance behavior of the radial distribution function is governed by long range spatial arrangements only; it does not depend on the volume fraction of size distribution of fibers. It follows that in the experimental distribution, the dip
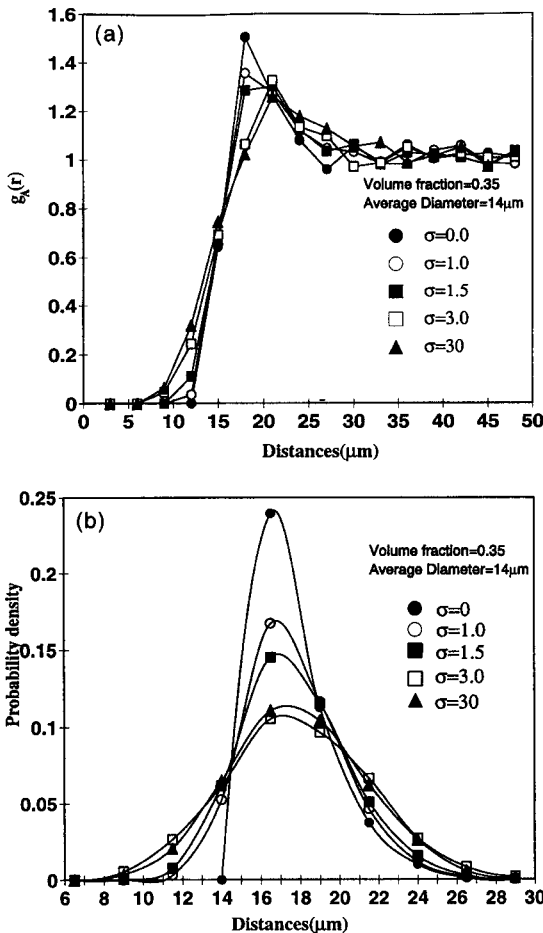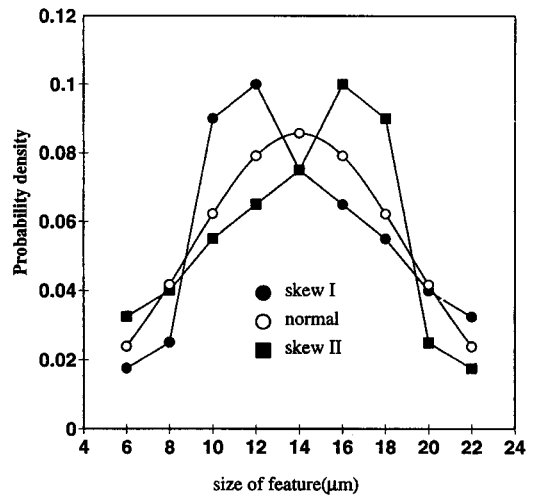

Fig. 9. Three distinctly different fiber size distributions having the same average size and same standard deviation, but different skewness.

below 1.0 in the distance range of 50–140 μm indicates that there are fiber poor regions at large distances from a typical fiber.

Figure 11(b) compares the experimentally measured nearest neighbor distribution with the corresponding distribution for the simulated hard-core random spatial arrangement having the same volume fraction and size distribution of fibers. These distributions also differ significantly. The peak heights are different, although the peak positions are approximately the same. The average nearest neighbor distance is 17 μm both in the CMC and the simulated hard-core random structure. Figure 12 depicts a typical microstructural field of the simulated hard-core random microstructure having the same volume fraction and size distribution as the SiC fibers in the CMC. Comparison of Figs 12 and 1 illustrates the differences between the spatial arrangements in the two microstructures.

From the comparisons of the radial distribution function and nearest neighbor distribution function of the SiC fibers in CMC and the simulated hard-core random structure, it can be concluded that: (1) the spatial distribution of SiC fibers is not uniform; (2) the spatial arrangement of the SiC fibers exhibits clustering at small distance ranges; and (3) the SiC fiber population exhibit scarcity of fibers (compared to hard-core random) at large distances. This is consistent with the qualitative microstructural observations (see Fig. 1).

MODELING OF NON-UNIFORM SPATIAL ARRANGEMENT OF FIBERS IN CMC

The present CMC was manufactured by a slurry infiltration type process [16]. In this process, resin binder and glass powder coated Nicalon (SiC) fibers are wound on a mandrel to form a tape. The tapes are stacked together, burned out to remove the resin

Fig. 8. Effect of the variation in standard deviation (σ) of the fiber size distribution on the spatial arrangement of the simulated hard-core fiber population. (a) Radial distribution functions of randomly distributed fiber centers with normal size distribution. (b) Nearest neighbor distribution functions of randomly distributed fiber centers.

binder, and then hot-pressed to densify the laminate. In this manner, the CMC is produced in the form of strips. Such a process may lead to alternate fiber-rich and fiber-poor regions along the thickness of the strip. A very low magnification micrograph of the CMC, shown in Fig. 13 illustrates these micro-structural variations along the thickness of the strip. There are no sharp boundaries between the fiber-rich and fiber-poor regions, but qualitatively the number density of fibers does appear to vary. These observations are consistent with the conclusions drawn from the analysis of the radial distribution function of the fibers in the last section.

The above discussion shows that it is reasonable to model the spatial arrangement of SiC fibers as alternate strips of fiber-rich and fiber-poor regions stacked together. It is assumed that the size frequency function of the fibers is the same in the fiber-rich and fiber-poor regions. The number densities of the fibers (and therefore, the fiber volume fraction) are different in the fiber-rich and fiber-poor regions. Let $(N_A)_f$ and $(N_A)_P$ be the number densities of the fibers in the fiber-rich and fiber-poor regions, respectively. Let λ_f and λ_P be the widths of the fiber-rich and fiber-poor strips. In each strip, the spatial distribution of fibers is

Fig. 11. Comparison of the experimentally measured spatial distribution functions of the SiC fibers in the CMC and the spatial distribution functions for the corresponding simu-lated hard-core random fiber population having the same volume fraction, number density and size distribution of fibers. (a) Radial distribution function. (b) Nearest neighbor distribution function.
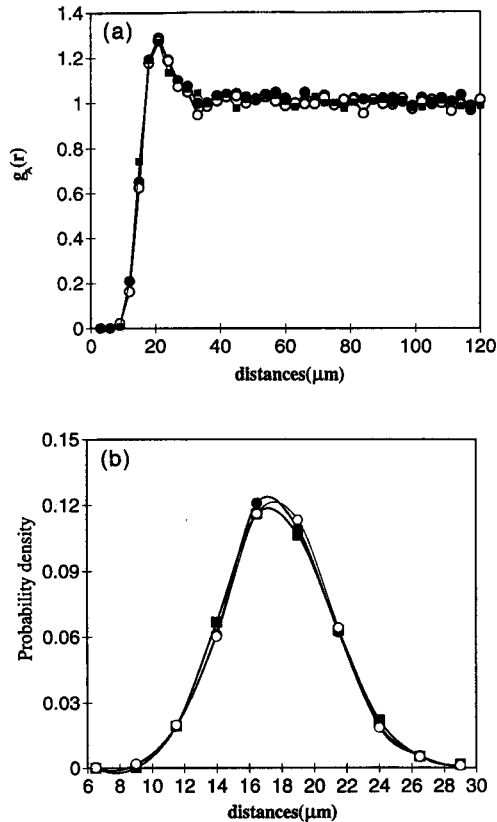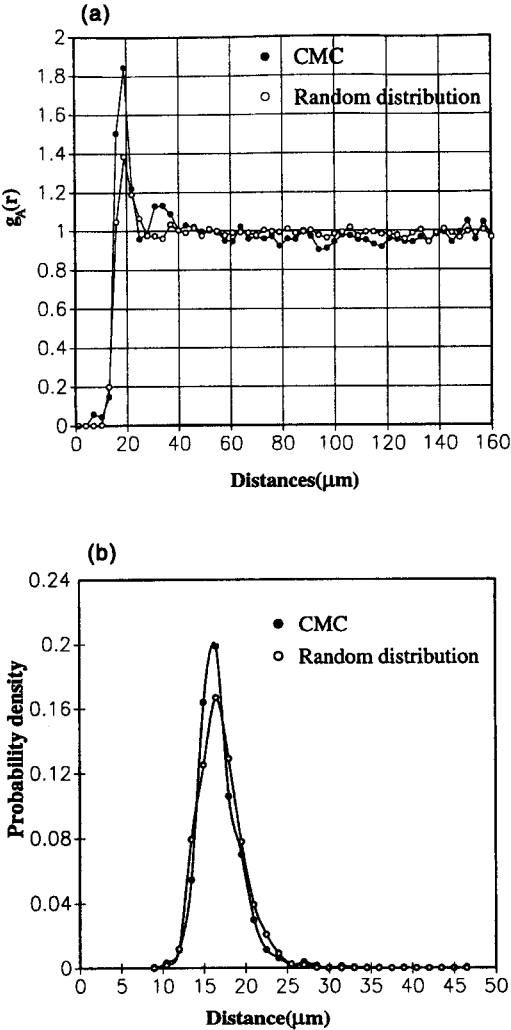

Fig. 10. Spatial distribution functions of simulated hard-core fiber populations having the three different size distributions shown in Fig. 9. Note that the spatial distribution functions are not sensitive to the skewness of the fiber size distributions. (a) Radial distribution functions. (b) Nearest neighbor distribution function.

assumed to be hard-core random; the non-uniformity is represented by different number densities of the fibers in the fiber-rich and fiber-poor strips. The model and parameters are schematically illustrated in Fig. 14. Let N_A be the overall average number density of the fibers, which is equal to 2.3×10^3 per $(mm)^2$ for the present CMC. One can write,

$$\lambda_f(N_A)_f + \lambda_P(N_A)_P = [\lambda_f + \lambda_P]N_A. \qquad (3)$$

Therefore, out of the four model parameters, $(N_A)_f$, $(N_A)_P$, λ_f and λ_P, only three can be varied independently once the overall average number density of fibers is specified. The four model parameters are essentially governed by the processing techniques and parameters. These model parameters govern the extent of non-uniformities in the spatial
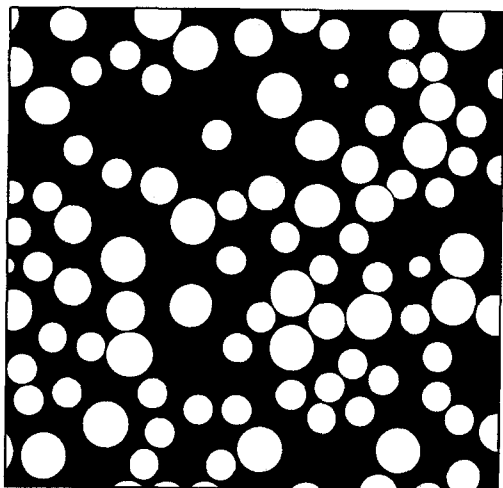
Fig. 12. A typical microstructural field of the computer simulated hard-core random microstructure having the same volume fraction, same number density and same size distribution of fibers as in the CMC.

Fig. 14. Schematic illustration of non-uniform distribution of fibers in strip model.

distribution, and thereby affect the mechanical properties of the composite. As there are no well-defined boundaries between the fiber-rich and fiber-poor regions in the composite microstructure, it is not possible to directly measure these model parameters. Therefore, the following trial and error scheme is used to estimate the model parameters. The values of the parameters are assumed and the microstructure is simulated. The radial distribution function and the nearest neighbor distribution of the fibers is calculated for the simulated structure by averaging over a large number of statistical realizations of the model. These spatial distributions are then compared with the corresponding exper-
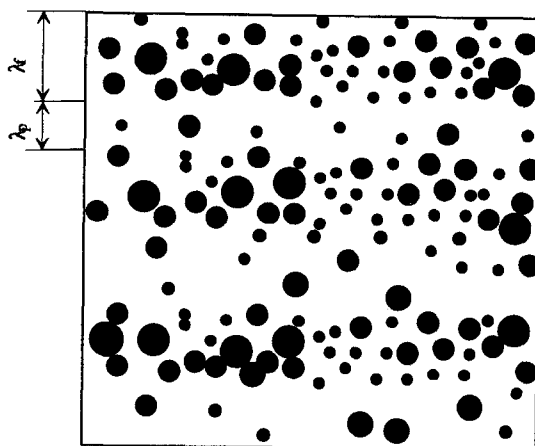
imentally measured spatial distributions for the CMC (Figs 5 and 6), and the model parameters are varied until the spatial distributions of the simulated structure agree well with the corresponding experimentally measured distributions.

Figure 15 compares the experimentally measured radial distribution function of the SiC fibers in the CMC with that for the computer simulated strip model. Observe that the first peak position and height in the two distributions match very well, and the two radial distributions match at the larger distances as well. Both the distributions show a dip below 1 in approximately the same distance range. The nearest neighbor distribution functions are compared in Fig. 16. The nearest neighbor distribution of the strip model matches perfectly with the experimentally measured distribution for the strip model. Figure 17
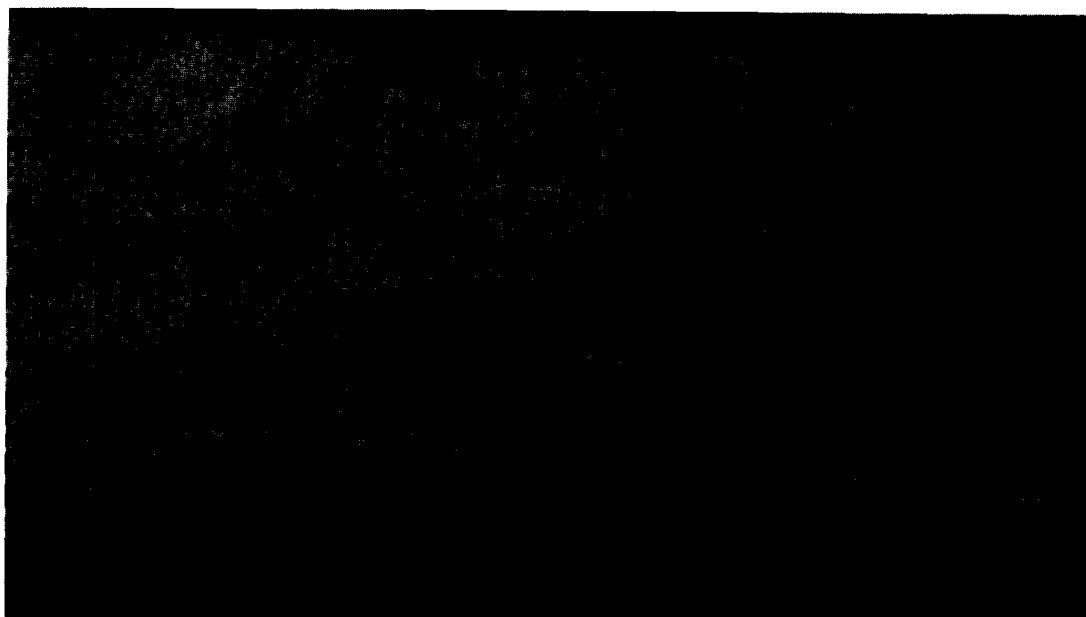

Fig. 13. Low magnification micrograph of CMC shows the alternate fiber-rich and fiber-poor regions.
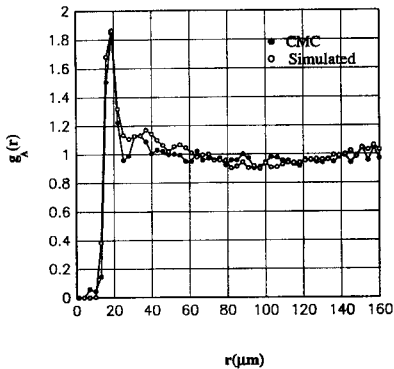
Fig. 15. Comparison of the radial distribution of the SiC fibers in the CMC composite and the simulated microstructure with strip model.

shows two typical microstructural fields of the *simulated* strip model microstructure at low and high magnification. Note that microstructures in Fig. 17 are *not* schematic; they are computer generated microstructures from the simulated strip model. Compare these computer simulated microstructures with Fig. 1, which depicts the actual microstructure of the CMC at the same magnifications. It is interesting to observe that the computer simulated and real microstructures look very similar.

The best agreement between the experimental and strip model spatial distributions is obtained for the following values of the model parameters: $(N_A)_f = 3500$ per $(mm)^2$, $(N_A)_P = 1100$ per $(mm)^2$, $\lambda_f = 80 \ \mu m$ and $\lambda_P = 75 \ \mu m$. The overall volume fraction, number density and size distribution of fibers in the strip model are exactly equal to those of the SiC fibers in the CMC. It may be concluded that the simulated microstructure of the strip model with these parameters is statistically equivalent to the microstructure of the CMC under investigation.
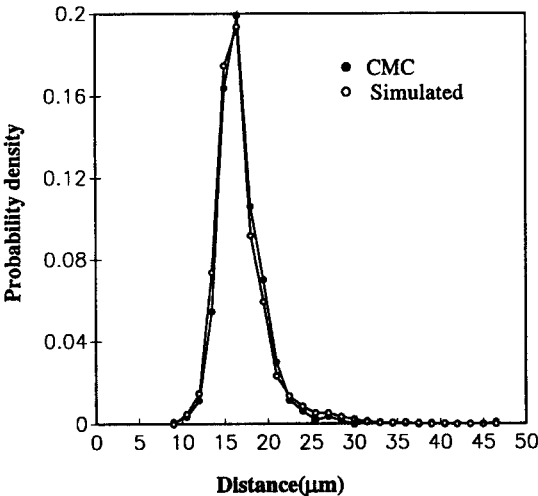

Fig. 16. Comparison of the nearest neighbor distribution function of the SiC fibers in the composite and the simulated microstructure with strip model.
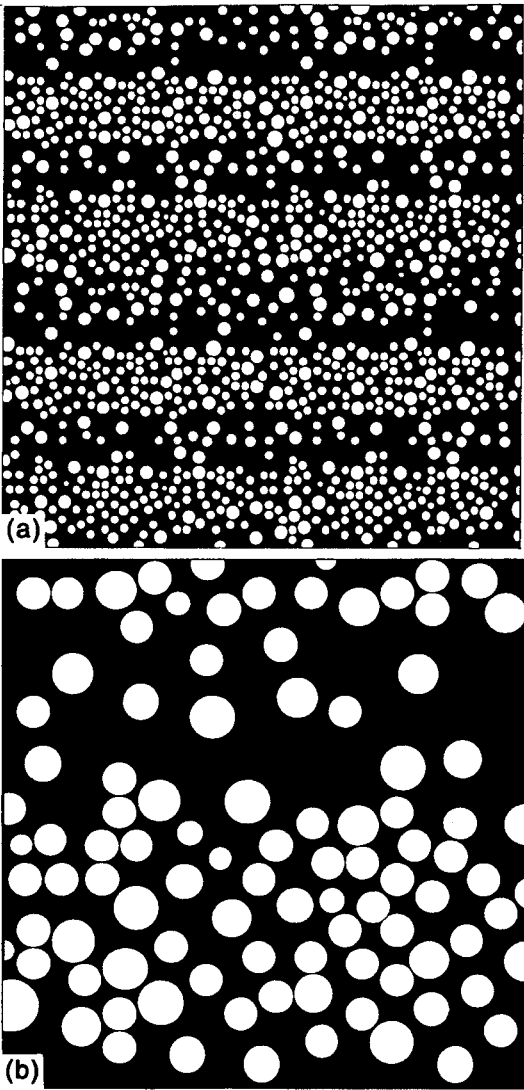

Fig. 17. Computer simulated microstructure with the strip model. Compare with Fig. 1 under the same magnification. (a) Low magnification (100 ×). (b) High magnification (500 ×).

Therefore, the model represents all the statistical attributes of the CMC microstructure: it has statistically the same spatial distribution of fibers, and the same average volume fraction, number density and size distribution of the fibers. The non-uniform microstructure of the CMC is therefore completely described in terms of a few numbers.

DISCUSSION

A quantitative model is developed for the non-uniform microstructure of a CMC containing unidirectional aligned Nicalon fibers in a glass ceramic matrix. The development of the model is based on detailed quantitative characterization of the non-uniform spatial arrangement of the Nicalon fibers and computer simulation of microstructures.

The methodology is quite general, and it should be applicable to any non-uniform microstructure of the unidirectional aligned fiber composite.

The "strip" model of three non-uniform CMC microstructure consists of alternate strips of fiber-rich and fiber-poor regions. Within each region, the fiber centers have a hard-core random spatial arrangement. It is assumed that the frequency size distribution of fibers (*not* number distribution) is the same in the fiber-rich and fiber-poor regions, and the size distribution of the fibers is normal (see Fig. 14). There are eight parameters in the model: fiber volume fraction, overall number density of fibers, average fiber size, standard deviation of the fiber size distribution, number densities of the fibers in the fiber-rich and fiber-poor regions [$(N_A)_f$ and $(N_A)_p$], and the widths of fiber-rich and fiber-poor strips (λ_f and λ_p). However, the last four parameters, and the overall average fiber number density are related through equation (3). Further, the volume fraction of the fibers is equal to their area fraction in the metallographic plane, and therefore, the volume fraction (V_v), overall average number density of fibers (N_A), average fiber size (R_a) and the standard deviation of the fiber size distribution (σ) are related as follows:

$$V_v = \pi N_A \{[R_a]^2 - \sigma^2\} \qquad (4)$$

Therefore, the model has six independent microstructural parameters. The parameters, $(N_A)_f$, $(N_A)_p$ and λ_p govern the non-uniformity of the spatial arrangement of the fibers, and V_v, N_A and R_a (how much, how many and how big) govern the metric attributes of the microstructure. The computer simulated microstructure with these six input parameters is statistically equivalent to the microstructure of the CMC. The microstructural model parameters are governed by the geometry and size distribution of the Nicalon fibers and the composite processing parameters, for a given manufacturing technique. It is important to emphasize that the spatial distribution of the fibers may vary from one batch to another, or from one plate to another plate in the same batch, or even from one region to another region in a given plate (these details will be presented in another contribution). These variations reflect the fluctuations in the process parameters. Therefore, the microstructural model parameters can be correlated to the process parameters, to develop very detailed processing–microstructure correlations. The results can be utilized to examine the changes in the microstructure when the processing parameters are changed.

The simulated microstructure can be used to generate the RVE for the micro-mechanical modeling of the mechanical response of the material. The simulated microstructure can also be utilized to determine the smallest RVE that is statistically representative of the material microstructure. For this purpose, the radial distribution function can be computed as a function of the volume of the simulated microstructure. The smallest RVE is the smallest simulated microstructural volume, whose radial distribution, fiber size distribution and fiber volume fraction are comparable to the corresponding experimentally measured attributes.

SUMMARY AND CONCLUSIONS

A digital image analysis technique is utilized for quantitative characterization of the spatial arrangement of Nicalon fibers in a glass ceramic matrix composite. These quantitative data and computer simulations are utilized to develop a quantitative model for the non-uniform microstructure of the CMC. The model requires six independent input microstructural parameters, and it generates a microstructure that is statistically equivalent to the microstructure of the CMC. The simulated microstructure can be utilized to generate the RVE for micro-mechanical modeling of the mechanical behavior of the composite.

REFERENCES

1. Brockenbrough, J. R., Suresh, S. and Wienecke, H. A., *Acta metall. mater.*, 1991, **39**, 735.
2. Sorensen, B. F. and Talreja, R., in *High Temperature Ceramic Matrix Composites, HT-CMC1*, ed. R. Naslain *et al.*, Woodhead Publishing Limited, Cambridge, U.K., 1993, p. 591.
3. Sorensen, B. F. and Talreja, R., *Mech. Mater.*, 1993, **16**, 351.
4. Pyrz, R., *Polym. Polym. Comp.*, 1993, **1**, 283.
5. Pyrz, R., *Mater. Sci. Eng.*, 1994, **A177**, 253.
6. Whited, W. and Gokhale, A. M., *Microstruct. Sci.*, 1994, **21**, 107.
7. Ripley, B. D., *Spatial Statistics*, John Wiley and Sons, London, 1981.
8. Ripley, B. R., *J. R. Stat. Soc.*, 1977, **39**, 212.
9. Schwartz, H. and Exner, H. E., *J. Microsc.*, 1983, **129**, 155.
10. Konig, D., Carvajal, S., Downs, A. M. and Rigaut, J. P., *J. Microsc.*, 1991, **161**, 433.
11. Chandrasekhar, S., *Rev. Mod. Phys.*, 1943, **15**, 86.
12. Louis, P. amd Gokhale, A. M., *Metall. Trans.*, 1995, **26A**, 1449.
13. Louis, P. and Gokhale, A. M., *Acta metall. mater.*, 1996, **44**, 1519.
14. Hanish, K. H. and Stoyan, D., *J. Microsc.*, 1980, **122**(II), 131.
15. Yang, S., Tewari, A. and Gokhale, A. M., *Developments in Materials Characterization Technologies*, ed. G. F. Vander Voort and J. J. Friel. ASM International, Materials Park, OH, 1996, p. 33.
16. Brennan, J. J., in *Fiber Reinforced Composites*, ed. K. S. Mazdiasni. Noyes Publication, Park Ridge, N.J., 1990.